Thermal reflectivity measurements of thin metal films

By: Elise Sophia Guarino, Supervisor: Peter Hadley

Research Report for the Marshall Plan Program

Contents

1 Abstract

The versatile structure and unique properties of metal-organic frameworks (MOFs) allows practical implementation for the design in real-world applications. To fully realize the potential of MOFs, it is essential to understand how their fundamental characteristics and properties impact on effective functionality. The initial focus of our investigation of metal materials, specifically within thin films, is studying their thermal transport properties such as thermal reflectivity and thermal conductivity. A promising technique to determine the temperature of the metal surface of the thin metal film is measure how much light reflects off it. This can be achieved by using the thin metal layers stacked on top of MOFs to act as thermometers to monitor temperature. To determine the thermal conductivity of the observed systems, it can be performed by taking a temperature measurement and monitor the change in optical reflectance as a function of temperature. When the thin film is subjected to heat by a laser pulse, the optical reflectance can be found as the sample cools. The properties and features of the thin metal films of interest will be studied via several thermal techniques such as ellipsometry and a form of pump-probe measurement called time domain thermal reflectance (TDTR).

2 Introduction

2.1 Metal Organic Frameworks (MOFs)

Metal-organic frameworks (MOFs) are a class of porous crystalline material that consist of bonds between transitional-metal ions and linked organic ligands. Their extremely high surface areas and unique diversity in structure design and tunability make them the ideal candidate for a multitude of applications allowing complete control of framework topology, porosity and functionality [1]. These hollow-structured materials are synthesized offering potential to create unique synergistic effects such as allowing certain gases within the pockets of their structures used for storage and separation, catalysis and sensing. MOFs have been extensively studied to have an in-depth understanding of their properties to allow precise modification of the material meeting specific requirements to be effective.

2.2 Thermal Properties of MOFs

In order to systematically control the certain properties of MOFs toward practical application, the temperature stability and behavior should be thoroughly studied. MOFs used in industrial applications are making progress to becoming efficient, although their heat management and thermal stability emerges important issues [2]. When subjected to extreme temperatures of a MOF compound, the thermal treatment process must be prioritized to avoid irreversible changes within its chemical and physical structure [3]. As these adsorbents are exposed to large thermal fluctuations, the release heat of absorption during charging needs to be constrained to avoid overheating the system. During the discharging phase, a temperature decrease occurs caused by the heat of adsorption which will increase the number of available adsorbates remaining in the pores of the

MOF. Based on the pressure swing adsorption (PSA), minimal temperature changes for these applications have a negative impact on their ability to perform efficiently [3]. Such processes assessed under heat present limitations of a given framework without influencing damage to the overall composition. For example, MOFs were realized for post-combustion carbon dioxide capture using a method called temperature swing adsorption (TSA), where they would use low energy penalty to influence the regeneration temperature using heat [4]. Most of these studies are limited to well known MOFs which are based on computational screenings of thermal properties as there are fewer studies carried that can test these properties experimentally. The practical implementation of MOFs for such applications has posed significant experimental challenges, particularly in relation to two critical properties: thermal reflectance and thermal conductivity.

2.2.1 Thermal Conductivity

Thermal conductivity is a crucial parameter for managing gas adsorption and gas storage as they are recognized as promising adsorbents capable in porous MOFs [5]. Heat dissipation and efficient thermal transport were observed to be the common issues that result in low thermal conductivities in these materials. The chemical diversity that make up the structure and porosity of MOFs effect significantly on the dynamics of bond strength in heat current fluctuations [6] which result in photon scattering. This is due to the choice of constituents that make up a MOF; created from the connection of metal ions with organic linkers through coordination ligands offering flexibility to structure pore volume and dimension. The hybrid cluster of compounds provide accessibility to many interactions between the organic and inorganic parts of its composition. Photon scattering occurs as a consequence within the pore cavities [7], demonstrating reduced propagation of excited photons. In several studies, it was investigated

that by using computational models to simulate that there was a decrease in thermal conductivity of cubic pore materials as the pore size increases due to the areal density of bond interaction [8]. These bond interactions serve as a means of thermal transport on the mobility of gas molecules (phonons) within the MOF. In the presence of adsorbed gas, the thermal conductivity of MOFs reduced significantly affecting the gas-crystal dynamics for these structures. Techniques for measuring the thermal conductivity in thin metal films are less common. These include scanning probe techniques such as scanning Joule microscopy, and photothermal methods where a probe laser spot is moved over a pump laser spot and a three-dimensional thermal model is used to determine film conductivity based on the signal phase as a function of the spot separation.

2.2.2 Thermal Reflectance

Another thermal property that needs to be dealt with in the context of thin-film based applications of MOFs is the thermal reflectance. It is a critical parameter that affect thin metal films' performance in a given application and several non-contact techniques have been developed for characterization which can be incorporated into manufacture use. Many of these developed methods are categorized to study the photo-thermal effects, such as frequency-domain thermoreflectance (FDTR) method and time-domain thermoreflectance (TDTR). The many advantages of using these non-contact methods can determine the film thickness, film density and film thermal conductivity. In one study, they used a FDTR approach to characterize thin metal films on low thermal diffusive substrates in conjunction with electrical conductivity measurements via Wiedemann-Franz Law [9]. The measurement approach allows a wide frequency range of thermal penetration depths with high accuracy, adjusted to the sensitivity for sub-micro thin films and equipped with a coaxial laser spot geometry for optimal alignment [9]. The signal strength in TDTR and FDTR measurements relies on the

combined influence of two factors. Firstly, the optical absorbance of the metal determines the extent of temperature elevation resulting from the heating effect of the pump beam. Secondly, the temperature dependence of the optical reflectivity governs the magnitude of intensity change in the reflected probe beam due to the induced temperature excursion [10]. Although the FDTR method has shown promising robust results, in this project we are more focused on using the TDTR method instead. While performing full TDTR scans, it creates spatially resolved thermal property maps over a region in the metal transducer/substrate interface as the two experimental variables can be further manipulated, the modulation f and the pump-probe delay time, enhanced to the sensitivity [11].

The measurements of the temperature dependence of the optical reflectivity, i.e., the thermoreflectance coefficient dR/dT, is determined using TDTR which is commonly used in ultrafast pump-probe experiments. Numerous studies conducted qualitative values of dR/dT in metallic elements and accurately predicted the thermoreflectance of a metal proved to be exceedingly challenging. A small increase in temperature can alter the optical properties introducing several factors: modifications in the electronic band structure caused by thermal expansion, shifts in phonon density affecting electron scattering rates, changes in the distribution of electron occupation close to the Fermi level and perturbing electron energy bands through electron-phonon coupling [12]. The thermoreflectance coefficient dR/dT of thin metal films significantly influenced by elastic strains due to heat expansion between the film and substrate of choice [12].

In this work, we will determine the temperature-dependent resistance of a thin film on different substrates to analyze a correlation with thermal reflectivity. The desired thin films are then deposited on substrates with plasma-induced Atomic-Layer Deposition (ALD). ALD techniques have been applied to deposit a wide variety of films that make it attractive for excellent conformality

and precise controlled thicknesses. The prepared samples used are thin films with a silicon substrate containing aluminium, gold, silver and a copper ring. The thin metal films were deposited on silicon substrate indicating promising clear current-voltage characteristics, feasible for electrical and thermal insulation. From a simple model of the reflectance for a thin metal film, it is assumed that electrons in a diffusive metal scatter frequently thereby taking the average over the scattering events at a certain period of time. The scattering time for electrons decreases when the temperature increases which is the reason why the reflectance is temperature dependent. Another factor involved in this process is that the electrical conductivity simultaneously change with temperature due to the change of the scattering time. This is important for measuring the temperature dependence of the electrical conductivity. Thus, thin metal films of interest with good thermal conductivities are desirable to impose temperatures that enhance the application performance during operation.

2.3 Applications Considered To Achieve Thermal Reflectance

Thermoreflectance techniques rely on measuring a material's change in reflectivity due to the change in its temperature. The applications of measuring temperature can be applied in modulated pump-probe measurement (TDTR) approaches, in combination of ellipsometry and four-point measurements to investigate thermal properties of thin metal films. In studying the properties of thermal reflectance and thermal conductivity of the observed material, a measurement of the temperature dependence of the reflectance of metal films as a function of wavelength can extract information that can be used to predict thermal reflectivity. In addition, determining measurements of temperature-dependent resistance and its dielectric characteristics of a thin film can be found on different substrates. The importance of finding the quantity of resistance is

crucial in finding if it is consistent with the quantity of thermal reflectivity.

In principle, we hope to achieve thermal reflectivity measurements of thin metal films which can be experimentally performed by the following methods considered: by applying a temperature gradient and measuring its flow of heat. The initial objective was if we use thin metal interface on the MOFs to act like thermometers, then it can quickly record temperature measurements. For the first goal of the project is to measure the temperature by monitoring the change in optical reflectance as a function of temperature by using an ellipsometer. Then by quantifying the change in reflectance, it is followed by involving the thin film subjected to induced heat by a laser pulse through the TDTR technique. As a result, the temperature would be measured by optical reflectance while we record the temperature decay. The thermal conductivity can be extracted as well. These are key steps in leveraging the thermal properties we are seeking and they are essential to overcome the experimental challenges in detecting thermal reflectance effectively. Thus, thin metal films of interest with good thermal conductivities are desirable to impose temperatures that enhance the application performance during operation.

2.3.1 4-Point Resistance Measurements

The four point probe is an efficient technique used to measure the sheet resistance of a thin layer of films or substrate in units of ohms thereby a current is driven through contact by two outer electrodes and reads the voltage by two inner electrodes. In a simple resistance measurement, the measuring wires and probe contact resistances are equally distanced and collinear to the sample. When a current I is in contact with the film conducting surface with a uniform resistivity ρ and the supplied current I spreads throughout the contact

uniformly inducing an electric field.

$$j = \frac{I}{2tr\pi}r \tag{1}$$

From this resistance measurement, the thickness of the film can be approximated as thin if the distance between the contacts is much larger than the thickness of the film. Conversely, the film's thickness is assumed to be thick if the distance between the contacts is much smaller than the thickness of the film.

The expression of the sheet resistivity is simplified to,

$$\rho = \frac{4\pi}{\ln(2)}\frac{V}{I}\Omega m \tag{2}$$

$$\frac{4\pi}{\ln(2)} = 4.53 \tag{3}$$

where V is the measured voltage and I is the force current.

From the above equation, the sheet resistivity is equal to the resistance of a square for a film.

When the equation is rearranged,

$$R = \rho\frac{L}{tW} \tag{4}$$

the sheet resistance is proportional to the resistivity of the material of a film divided by its thickness.

2.3.2 Ellipsometry

Ellipsometry measures the change in polarization as the incident radiation reflects or transmits interacting from the material structure of interest. To measure thermal reflectance, it can be done by an optical technique called ellipsometry which allows us to further analyze film thickness and optical properties of

thin films using an ellipsometer. The primary interest of ellipsometry is how p- and s- components of a polarized light change due to reflection or transmission in relation to each other [13]. The polarization change is denoted as an amplitude ratio, Ψ, and the phase difference, Δ. This change in polarization is denoted in the equation:

$$\rho = \tan(\Psi)e^{i\Delta} \tag{5}$$

When these components are calculated using Fresnel equations, they describe the amount of light reflected and transmitted at an interface between materials:

$$r_p = \frac{E_{rp}}{E_{ip}} = \frac{n_t \cos\theta_i - n_i \cos\theta_t}{n_t \cos\theta_i + n_i \cos\theta_t} \tag{6}$$

$$t_p = \frac{E_{tp}}{E_{ip}} = \frac{2n_i \cos\theta_i}{n_t \cos\theta_i + n_i \cos\theta_t} \tag{7}$$

$$r_s = \frac{E_{rs}}{E_{is}} = \frac{n_i \cos\theta_i - n_t \cos\theta_t}{n_i \cos\theta_i + n_t \cos\theta_t} \tag{8}$$

$$t_s = \frac{E_{ts}}{E_{is}} = \frac{2n_i \cos\theta_i}{n_i \cos\theta_i + n_t \cos\theta_t} \tag{9}$$

where r represents Fresnel reflection and t represents Fresnel transmittance coefficients used to calculate interference from each contributing beam. Light reflects and refracts at each interface, leading to a superposition of multiple beams in a thin film. Interference between beams depends on relative phase and amplitude of the electric fields. The film phase thickness is defined:

$$\beta = 2\pi \frac{d_1}{\lambda} n_1 \cos\theta_1 \tag{10}$$

By inputting the values into a model analysis, for example, the Forouhi Blommer Model, can determine unknown optical constants and/or thickness parameters. If the values are unknown, then an approximated value is given for calculations. Through regression analysis, the best approximation between the model and experiment is achieved by use of an estimator such as Mean Squared Error (MSE), used to calculate the difference between curves corresponding to the 'global' minimum reached.

As a result, analyzing the change of polarization of light can yield information and characterize film thickness for micro-layer stacks of the material that are thinner than the wavelength of the probing light itself. For example, the reflected intensity and ellipsometric Δ for two thin oxides on silicon show high sensitivity of intensity in Δ although their reflectance are relatively the same. This is determined from film thickness that is measured more than 100 nm (for metals), as interference oscillations are more difficult to resolve largely affecting the path length of light allowed to travel through the film. Film thickness is dependent on optical constants, n,k and the refractive index, contributing to the delay between surface reflection and light traveling through the film.

Two corresponding values are used to describe optical properties determine how light interacts with a material. Such values are represent the complex dielectric function ϵ:

$$\epsilon = \epsilon_1 + i\epsilon_2 \tag{11}$$

with the following relation between an index (n) and extinction coefficient (k) introducing the complex refractive index $\tilde{n}$ of a metal film:

$$\tilde{n} = n + ik \tag{12}$$

The index of refraction n of a material is written as a complex and the

extinction coefficent k determines the attenuation of light intensity as it propagates through a material. Metals that exhibit high extinction coefficients render them effective reflectors.Insulators possessing small values of k are considered less proficient reflectors. Other optical constants that are considered for a diffusive metal by finding the square root of the dielectric constant ϵ_r when equations 11 and 12 are related to arrive at the following equation:

$$\sqrt{\epsilon_r} = n + ik \tag{13}$$

The temperature coefficients describe the real and imaginary parts of the index of refraction, dn/dT and dk/dT if we relate them to the dielectric constant (also the thermoreflectance coefficient, dR/dT). We can further derive reflectance R at normal incidence which is given by:

$$R = \frac{(n-1)^2 + K^2}{(n+1)^2 + K^2} \tag{14}$$

At non-normal incidence, polarization of the incident is dependent upon the amount of light reflected at an interface, where the p- and s- components become prominent. The reflection coefficient of light polarized in the plane (p-polarization) is shown in Eq. 6 while the reflectance of s- polarized light is given by Eq.8. For cases of n_i ¡ n_t and n_i ¿ n_t against the angle of incidence, s polarization will increase at all angles of incidence whereas p polarization will approach 0 at Brewster's angle ($\theta_B = \tan^- 1\ \frac{n_i}{n_t}$). Total internal reflection occurs when n_i is larger than n_t at the critical angle. If n_i is smaller than n_t, a portion of the incident light would undergo transmission out of the material, while the remaining light would be reflected back into it as governed by the Fresnel equations.

The plasma frequency ω_p describes the frequency dependent electrical con-

ductivity, critical for determining reflectance of the desired metals. Reflectance is denoted as a function of frequency ρ in units of plasma frequency (rad/s) and the plasma frequency is measured at which the metal is absorbing light ($\omega = \omega_p$), reflecting (($\omega < \omega_p$) and transparent ($\omega > \omega_p$).

The index describes the phase velocity of waves traveling in a material at the speed of light c in vacuum. The frequency remain constant when light travels in a material with a higher index. In electromagnetic waves, the extinction coefficient k describes the exponential loss of energy in relation to the absorption coefficient α:

$$\alpha = \frac{4\pi k}{\lambda} \tag{15}$$

The amplitude of the waves squared is proportional to the exponential decay of light intensity according to Beer's Law:

$$I(x) = I_0 e^{-iax} \tag{16}$$

2.3.3 Time Domain Thermal Reflectance (TDTR)

Thermal conductivity can be investigated with pump-probe measurements, a specific type of pump-probe called time domain thermal reflectance which can be used to obtain information on picosecond timescales. In this case, a pump-beam is used to thermally excite the interface of a sample at frequency f. The variation in the intensity of a reflected probe beam depends on the temperature change at the surface as a function of either f or the pump-probe delay time. TDTR uses short pulses to monitor the thermoreflectance decay as a function of delay time and also as a function of the phase shift induced after heating at f [11]. The general principle entails the investigated object is heated by pump pulse, generating excitation in the sample. Based on a time delay, a weak probe pulse probes the sample and its reflectance is measured. In the

pump and probe beam paths, the generated pump beam is focused through a chopping disk that halves the laser repetition rate. When two probe pulses achieve the desired ratio, they are then averaged. Within the transmitted pump beam pathway, it is blocked in order to measure the pump signal's influence on the probe intensity which is detected and digitized by the photodetector. After modifying the pathways, a TA scan involving a pump-probe delay is set with an adjustable delay stage yielding a time-step resolution. As a result, the transient absorbance independent of the pump signal is subtracted from the pump-probe transient absorbance to eliminate other light interference. The data is obtained by monitoring the probe signal after its excitation as a function of the time delay with respect to the change of reflectance.

Through this alternative application of the TDTR, thermal properties can be acquired from the thin film material of interest or very small crystals (up to hundreds of nanometers thick). It is a method that is considered when investigating thin films of only a few microns thick. The test setup is based on a pulsated laser subjecting localized heat of a material creating localized temperature increase, thereby inducing thermal stress. At the surface interface, the change of reflectance can be utilized to derive thermal conductivity and thermal conductance with respect to temperature. These two parameters can be obtained independently based on delayed times and the data received can be compared to a thermal model.

Since MOFs are extremely sensitive to forms of heat process, we would like to avoid further damage on the samples without using the TDTR method. Applications conducted to avoid permanent impairment was used such as transient absorption microscopy (TAM) detection for organic thin films of squarine achieved a similar experimental process. This implementation simulates a TDTR pump-probe measurement, utilizing pump-probe and probe only pulse

sequences recording at a femtosecond resolution monitored by a photodetector system detecting transmission changes by alternating the population states within the material. By varying time delays between pump and probe pulses, the population decay was observed.

3 Methods

In this project, the primary goal is to calculate the thermal reflectivity of thin metal films that were experimentally performed by applying a temperature gradient. To reiterate, we proposed that these thin metal films will act as thermometers that can be used to measure temperature. Thereby, the first objective is to determine the resistivity and resistance using four-point measurements.

The following method eliminates the contact resistance from the measurement by supplying a uniform current through the outer electrodes and measures voltage through the inner electrodes. Voltage and current were measured using Keithley 2600 Series Sourcemeter from which resistance was calculated as a function of temperature. The prepared samples used are thin films with a silicon substrate containing aluminium, gold, copper and silver. The thin metal films deposited on silicon substrate indicate promising clear current-voltage characteristics and is feasible for electrical and thermal insulation. The thickness for each thin film sample was measured using an optical profilometer, that quantitatively determines the surface profile determined by step heights and surface roughness. The profilometer profiles approximately 10 nm over several small sections across two etchings on the surface, these measurements were then averaged. It was found that each of sample's film thickness were found to be approximately around 40 nm with an uncertainty of 0.86 nm.

Each sample was then placed in a Vötsch VT4002 climate chamber with the sourcemeter attached, subjected under a temperature range from 20 C° to 60 C° calculating temperature dependence of the resistivity. For each temperature, a waiting time of 300s between each measurement was implemented ensuring a constant temperature, to stabilize an approximated value that can be compared to the literal value. The chamber was operated closely monitored at this temperature range during the purge time. These measurements were regulated

using a python code with 100 iterations being done for every temperature step, averaging the resistance value returning each temperature step and rendered a graph of resistance as a function of temperature. As the chamber reaches 60 C°, it returns to the room temperature ending the python code. As an additional step, another measurement was done with a decreasing temperature range to show consistency with an increasing temperature trend.

For the second objective, the samples were then tested using the J.A. Woollam M-2000 ellipsometer to monitor the change in optical reflectance as a function of temperature. Primarily it purposes thin film characterization and optical constants: n and k, Ψ, Δ, real and imaginary parts of reflectivity ρ and the square root of the dielectric constant ϵ. The samples were recorded with a wavelength range of 371.5 nm to 999 nm at 20 C° to 60 C° at a duration of 1320s. They were then technically adjusted and centered at an angle of incidence 70°. After the ellipsometer reached the final temperature, it cools returning to room temperature. The experimental data extracted from the ellipsometer program produced spectroscopic ellipsometric (SE) data for Ψ versus Δ, n versus k coefficients, real ρ versus imaginary ρ and dielectric constants ϵ_1 versus ϵ_2 as a function of the set wavelength range. The optical constants were determined by fitting the ellipsometer parameters in the wavelength region from 371 nm to 999 nm. Data analysis was further calculated by using an Excel program to find each optical constant. We hope to find a correlation between the optical properties we predict from the 4-point measurements and compare those predictions to the ellipsometry measurements.

4 Results and Discussion

Thermoreflection measurements were made on thin metal films of Al, Au, Ag and Cu at a temperature range from 20 C° to 60 C°. The data yielded was further evaluated to predict the optical properties from the 4-point measurements and then compare those predictions to the ellipsometry measurements. Additionally, we demonstrate that there is a correlation between the experimental values that was obtained with literature values to see if they are in good agreement. For the first part of this work, we demonstrated 4-point measurements on the following samples tested regulated to calculate the temperature dependence of resistivity at each temperature step at an increasing temperature of 20 C° to 60 C°. In the second part, we examined the spectral curves of the ϵ_1 and ϵ_2, refractive index (n) and extinction coefficient (k) of the thin metal films tested within the wavelength region of 371 nm to 999 nm, as well as a summary of optical coefficients performed under ambient conditions.

The following table describes the film optical constants calculated from experimental data:

Sample	Ψ	Δ	ρ	$\sqrt{\epsilon_r}$
Aluminum	11.82	168.15	1.299	1.74
Gold	37.56	98.17	4.429	1.82
Silver	42.84	114.66	20.80	1.84
Copper	30.53	87.41	1.06	1.74

Table 1: Optical film constants with averaged values.

The dielectric function from equation 12 can equivalently written in terms of sin and tan functions at an angle of incidence of 70°:

$$\epsilon_r = \sin^2\theta_i[1 + \tan^2\theta_i \frac{1-\rho}{1+\rho}] \tag{17}$$

By using equation 5 to relate to equation 16, the corresponding values of

ψ and Δ were calculated from data analysis. Furthermore this relation is then related to the dielectric equation 11 and 13 to arrive at the following equation:

$$= \frac{sin(2\psi)\cos(\Delta) + i(\sin(2\psi)\sin(\Delta)}{1 + \cos(2\Psi)} \tag{18}$$

where reflectivity ρ can be conversely written as ρ_{real} and ρ_{img} can be shown in terms of Δ and ψ:

$$\rho = \rho_{real} + i\rho_{img} \tag{19}$$

$$\rho_{real} = \sin(2\psi)\cos(\Delta) + (\sin(2\psi)\sin(\Delta)) \tag{20}$$

$$\rho_{img} = \sin(2\psi)\cos(\Delta) + i(\sin(2\psi)\sin(\Delta)) \tag{21}$$

4.1 Aluminium

Aluminum is a widely used metal due to its excellent properties such as high electrical and thermal conductivity, low density, and good corrosion resistance. The temperature dependence of the resistance of aluminum indicates that the linearity of experimental values is considerably more prominent than that of accepted values. Specifically, the accepted value for the resistivity of aluminum is 2.65 Ω m, whereas the average experimental resistivity is 1.65 Ω m, resulting in a difference of 1 Ω.

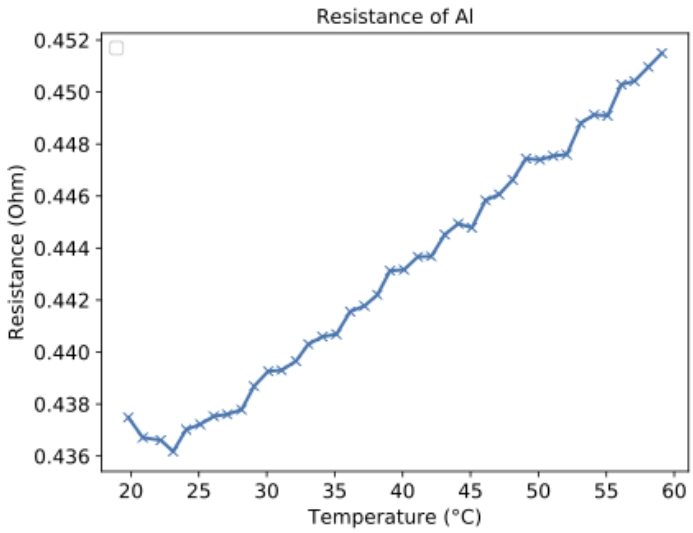

Figure 1: Resistance of a thin film of aluminium on silicon substrate.

Fig. 1 suggests the tested sample of a thin film of aluminium on a silicon substrate performed at an increasing temperature with an average resistivity of 0.1654 Ω cm. It is observed that there is an increase of aluminium film absorbing light gradually over a wide temperature range, thereby the data oscillations of surface reflection shown were suppressed. The resistance of inter-band absorption in aluminium suggests it has a poor thermal contact resistance as an

metallic interface due to its low melting point of 600 C° [16].

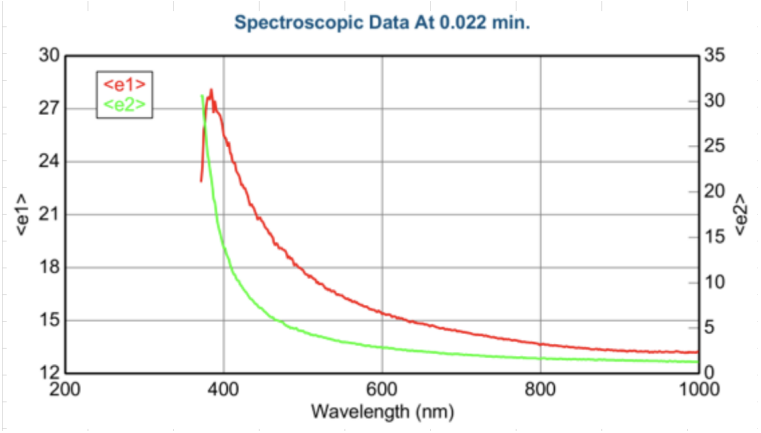

Figure 2: ϵ_1 and ϵ_2 spectra of aluminium.

Fig. 2 shows the ϵ_1 decreases gradually with increasing wavelength similar to ϵ_2 as follows, indicating a loss of photon energy was observed.

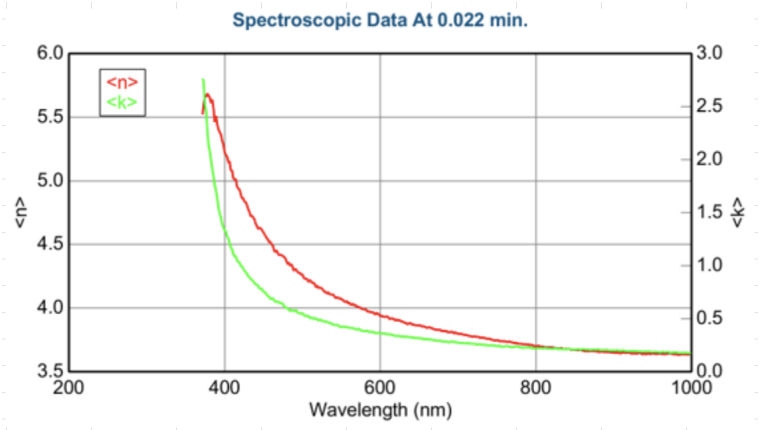

Figure 3: Resistance of a thin film of aluminium on silicon substrate.

Notably, both n and k exhibit a prominent decrease as the wavelength increases, following a similar trend when calculating the dielectric parameters depicted in Figure 3. These decreasing values indicate significant absorption of

the thin film within the wavelength region. The observed rise in the refractive index is attributed to fundamental band gap absorption.

In addition to the resistivity, other optical properties of aluminum as a function of temperature is also important to consider. In the aluminum sample analyzed, the averaged refractive index (n) of 4.113 gradually decreased with an extinction coefficient (k) of 0.406 at 550 nm. The experimental dielectric constant value of 1.74 falls within the range of the accepted value of 1.6 - 1.8.

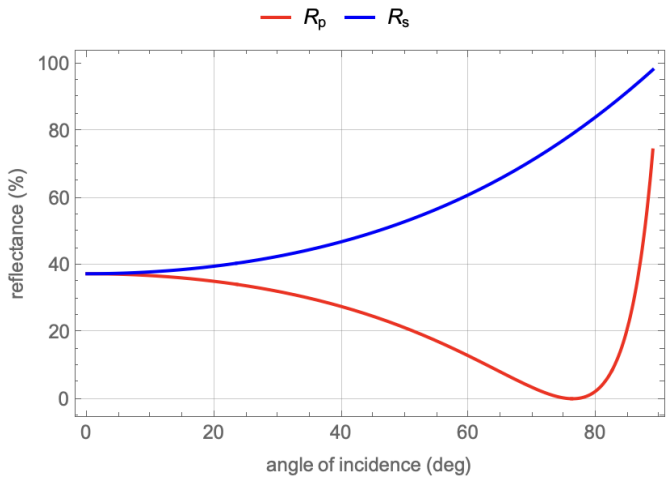

Figure 4: Reflectance of a thin film of aluminium on silicon substrate by Wolfram Demonstration.

In Fig. 4 we observed the reflectance of aluminium as a function of angle of incidence upon reflection generated by Wolfram Demonstration [15]. Considering the reflectance R_s it gives us a reflectance of 65 percent that is slightly below than the literature value ranging 75 - 95 percent [16]. Reduction of reflectivity for p-polarized light was significant approximating close to ¡ 5 percent. As the Fresnel amplitude and phase are changed due to temperature rise, we calculated $\epsilon = 2.028 + 0.637\text{i}$ which corresponds to $\tilde{n} = 4.113 + 0.406\text{i}$. Our findings are

significantly lower when we compare ñ value to the Wolfram graph [15], where ñ = 0.925 + 6.399i. This is probably due to metal films often have different ϵ_r values due to conditions from manufacture and frequent use over time which result in defects, changes in surface roughness and contamination. In this case, ϵ can be best fitted for the reflectivity curve of the p-polarized light using the complex dielectric constant as a parameter.

When comparing the optical constants obtained from data analysis to the Lorentz-Drude model, our findings do not agree with the literature review. At approximately 550 nm, (n) of 0.965 with coefficient (k) of 6.458 [17] confirming that these estimations are close to Wolfram values [15]. Other literature parameters include $\rho_p = 0.79656$ and $\rho_s = 0.97045$ with a slight linear trend of above 95 percent reflectance but still shows similar graph as Fig. 4. A n value of 6.458 exhibiting high reflectivity means that aluminium should be a remarkable metal candidate induced under thermal heating conditions, although our data is not in agreement. However, the reflectance of a diffused surface can be significantly improved by deposition of a polymer smoothing layer to prevent further defects. Additionally, the average rate of change in thermal-reflectance response depicted as high at elevated temperatures for aluminium which resulted in a large thermal expansion, suggesting it does not retain its durability under high heating conditions [18]. These results also support the assertion that the low reflectance is due to degradation by handling and environmental damage.

4.2 Gold

It is observed that there is direct relation between the decrease in resistance and film thickness of the sample increases, thereby approaching bulk resistivity exceeding the critical value [14]. In Fig. 4, the second sample tested was a thin film of gold on a silicon substrate performed with an average resistivity of

0.4256 Ω cm.

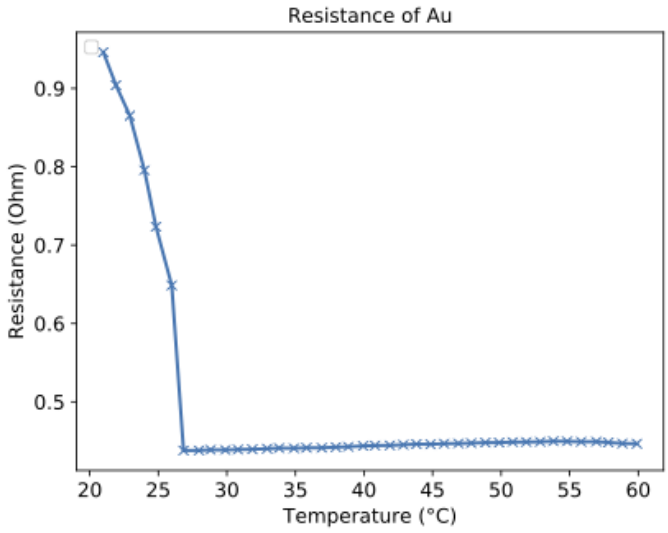

Figure 5: Resistance of a thin film of gold on silicon substrate.

As shown in Fig. 4 a sharp decreasing trend as the temperature increased may be due to the rough surfaces, resulting in more scattering and decreased interaction of charged carriers in free mean path. The exhibited signs of degradation in the sample at elevated temperatures may also present impurities, modifying the electronic band structure of the gold and its electrical conducting properties when 4-point measurements were being done simultaneously inside the climate chamber [20]. The expression for the temperature at which the resistance changes from metal behavior to non-metal behavior was exceptionally notable when it approaches 25 C° and then declining sharply, as it stabilize at low resistances until it reaches the maximum temperature of 60 C° before cooling at room temperature [21].

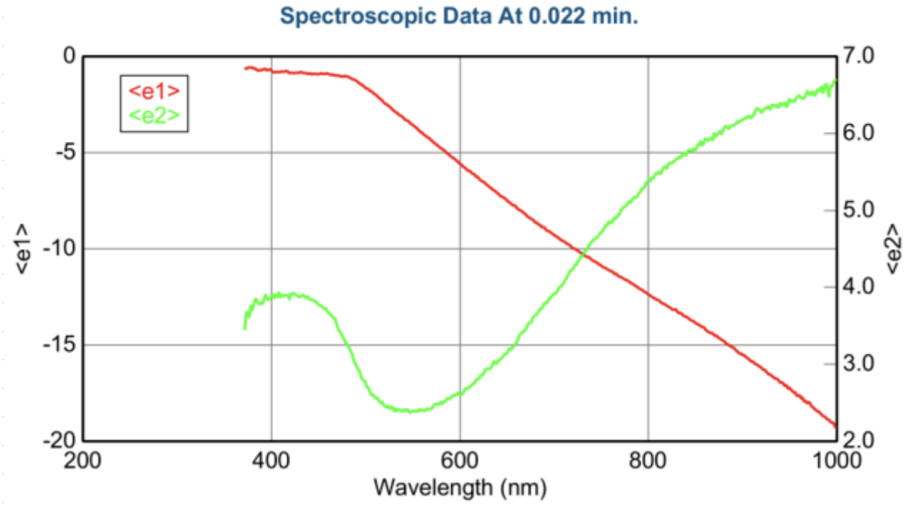

Figure 6: ϵ_1 and ϵ_2 spectra of gold.

As we can see in Fig. 5, the real part of dielectric function ϵ_1 significantly change at higher temperatures at approximately 472.5 nm, while the imaginary part ϵ_2 increases monotonically. The increase in ϵ_2 behavior can be further understood from the increased scattering rates of free electrons that depends with increasing temperature and on the interactions between electron-photon [21].

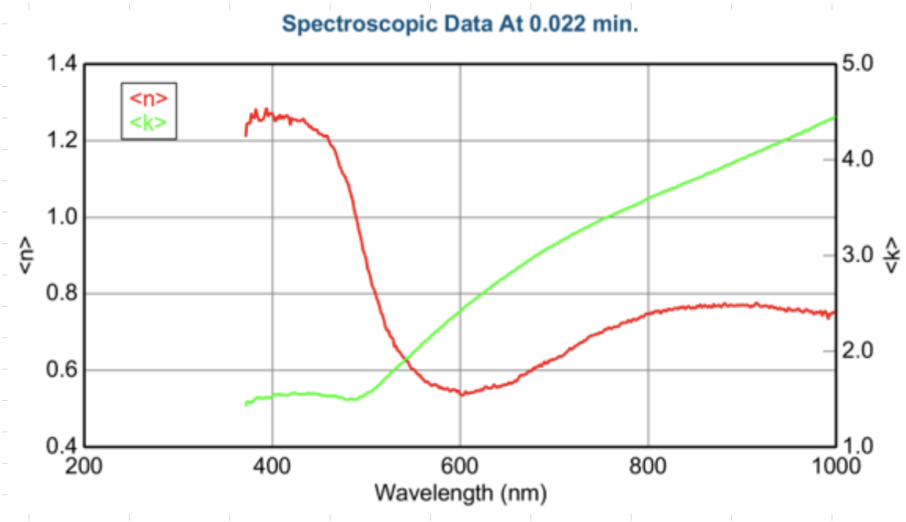

Figure 7: ϵ_1 and ϵ_2 spectra of gold.

In the gold sample, the refractive index n of 0.605 gradually decreased with extinction coefficient k of 1.993 considering the set wavelength of 550 nm. When the temperature cools to room temperature, the likelihood of ϵ_2 behavior would slightly decrease. After the heating treatment, it is revealed that the surface roughness increased with surface scattering thereby noting that the film will show some permanent degradation, which will be an issue when measuring future testing under same experimental conditions which may lead to discrepancies and errors in the data.

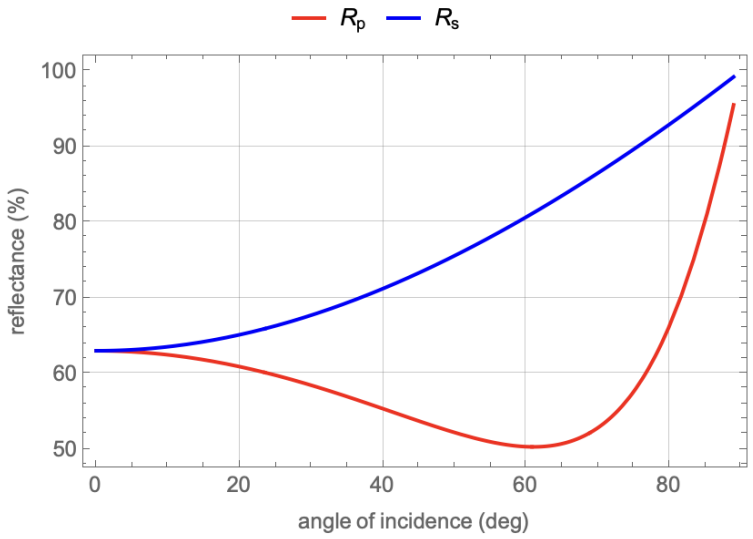

Figure 8: Reflectance of a thin film of gold on silicon substrate.

As we can see in Fig.8, the reflectance percent at incident angle 70 is approximated to be 90 percent considering R_s. As the Fresnel amplitude and phase are changed due to temperature rise, we calculated $\epsilon = 0.336 + 0.637\text{i}$ which corresponds to $\tilde{n} = 0.605 + 3.972\text{i}$. Our findings are significantly lower when we compare $\tilde{n}$ value to the Wolfram graph [15], where $\tilde{n} = 0.421 + 2.345\text{i}$. When we based our optical constants obtained from data analysis to the Brendel-Bormann model, our findings are within reason to agree with the literature review [17]. At approximately 550 nm, (n) of 0.663 with coefficient (k) of 0.910 [17] confirming that these estimations are close to Wolfram values [15]. Other literature parameters include $\rho_p = 0.677$ and $\rho_s = 0.922$ where it is depicted at above 90 percent reflectance, simulating a similar model with Fig. 8. Gold would make as an other ideal metal candidate for studying thermal reflectance due to its relative high ρ_s, this phenomenon could potentially be attributed to the fact that excited electrons resulting from electron-phonon coupling may induce more

substantial alterations in the optical properties compared to a simple excitation. [21].

4.3 Silver

Silver has been extensively studied as a potential material for large scale integration due to its bulk electric resistivity (1.57 $\mu\Omega$m at room temperature) and higher electro-migration resistance than aluminium [20]. However, it has been addressed that agglomeration of silver occurs during thermal annealing, exposing the substrate thus reducing the energy in the system. This has been known to be a disadvantage for silver thin films which largely affects the reliability for measuring thermal stability. We proposed to measure the electric resistivity using four-point measurements but they were not conducted as the sample were not readily available from the beginning of the project. Therefore we can infer that there would be a linear correlation between resistance and increasing temperature, similar for metals like aluminum. In our findings, silver was calculated to have the highest reflectivity ρ of 20.8 over the visible wavelength range, making it an exceptional good conductive metal. An investigation of silver thin films on silicon was found to be unstable, the thermal stability was the greatest when the thickness was above 85 nm [23]. Since the film was measured to be 40 nm, we can discern that the resistivity of thinner films would be shown higher from room temperature until 60 C° due to an increase in surface area of electron scattering. There is a direct correlation between minimizing surface area with increased resistivity because of the voids that form grow throughout the film and the agglomeration process [23].

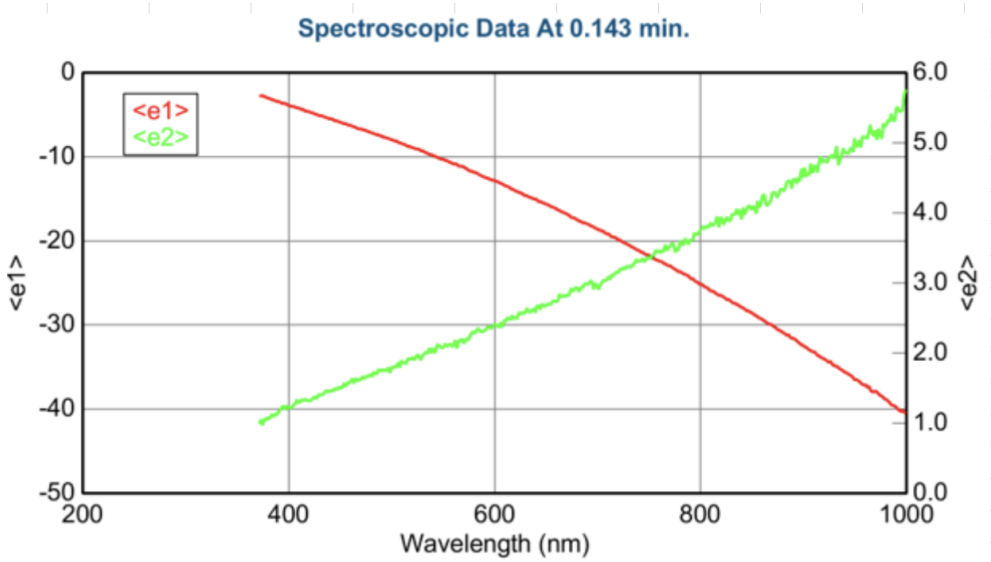

Figure 9: ϵ_1 and ϵ_2 spectra of of silver.

Fig. 7 depicts ϵ_1 in a decreasing trend whereas ϵ_2 value increased with increasing photon energy.

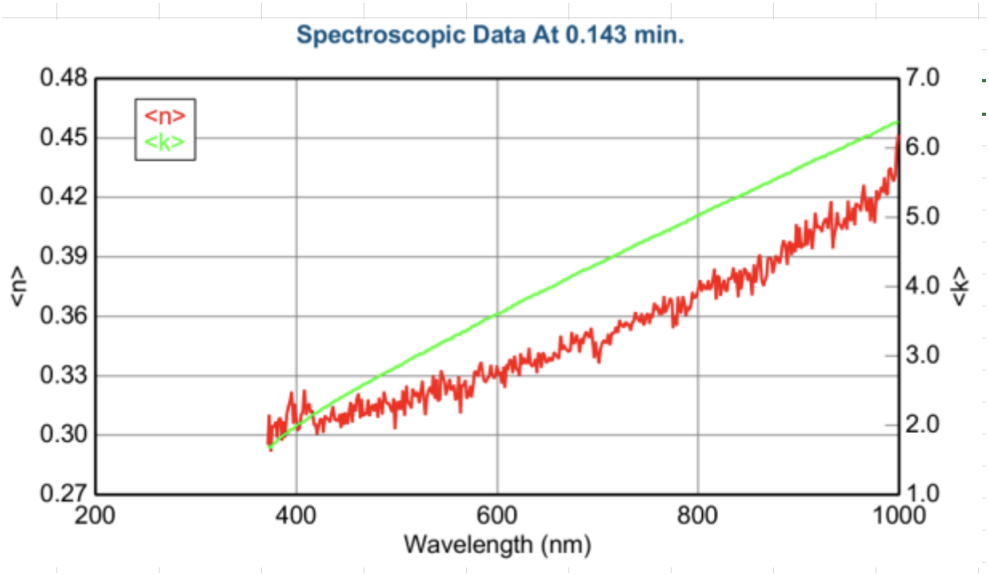

Figure 10: The spectra curve of refractive index and extinction coefficient of silver.

The optical properties of silver thin films are heavily dependent on their micro structure, which can be tailored through deposition and annealing processes. The refractive index n of 0.326 gradually increased showing a linear regression with extinction coefficient k of 3.240 for silver at 550 nm were calculated from the data analysis. These values are in agreement with silver's excellent characteristic of high reflectance, in addition to imparting high thermal stability and low electrical resistivity. In a previous study, the deposition of silver films with other metals, in this case aluminium was used for deposition, helps suppress agglomeration but also influences its physical and optical properties [24]. Aluminium was primarily selected ideal for realizing thermally stable silver film possessing high optical properties [24]. The total composition of the film's resistance show a negligible level of diffused but high reflectance. In addition, the influence of the deposition of aluminium nanolayer on silver films show that the

Al/Ag bilayers' thickness was 1 - 3 nm close to one silver layer [23].

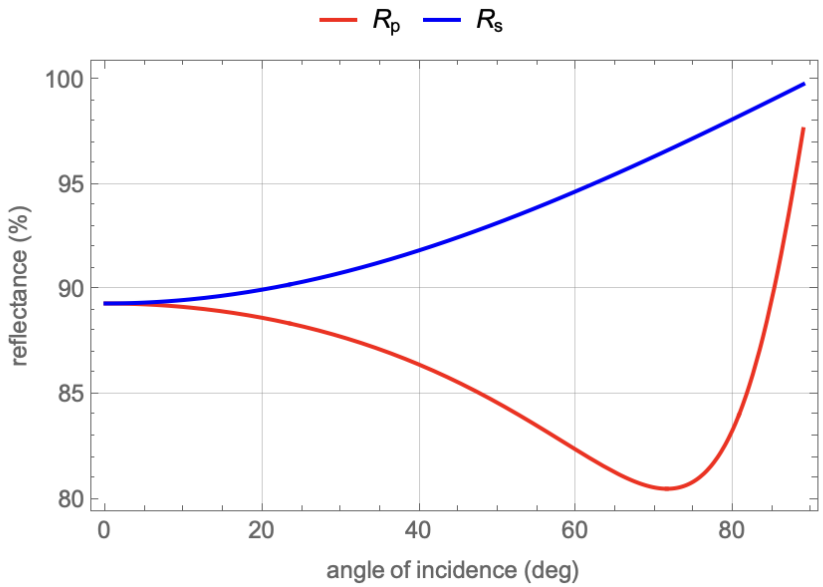

Figure 11: Reflectance of a thin film of silver on silicon substrate.

In Fig.11, it depicts a highest reflectance percent at incident angle 70 is approximated to be greater than 95 percent when we consider R_s. According our investigation, our data for $\epsilon = 0.106 + 40.947$i with respect to $\tilde{n} = 0.326 + 3.240$i was calculated. Our findings of $\tilde{n}$ value were found to be less then that the Wolfram graph [15] value reported of $\tilde{n} = 0.145 + 3.190$i. As we compare the optical constants obtained from our data to the Brendel-Bormann model [17], we found that our the $\tilde{n}$ value did not agree with the literature value. It was noticeable to find since experimental $\tilde{n}$ value was almost half of the literature value although our k coefficient was negligible. At approximately 550 nm, (n) of 0.145 with coefficient (k) of 3.190 [17] confirms an exact estimation to the Wolfram values [15]. Other literature parameters include $\rho_p = 0.906$ and $\rho_s = 0.983$ whose graph is similar to Fig. 11. The exact value for ρ_s is significantly

high with a 98 reflectance percentage, highly effective as an efficient reflector than aluminium [16]. The implications of silver being a great transmitting material for thermal reflectance due to its high concentrated light transmission and low absorbance under

4.4 Copper

It has been studied extensively that high purity copper, along with high purity aluminium, are important materials that offer large bulk thermal conductivity at highly elevated temperatures up to 4K [25]. In addition, copper can measure significant bulk thermal conductance at low temperature, regulating a high thermal resistance.

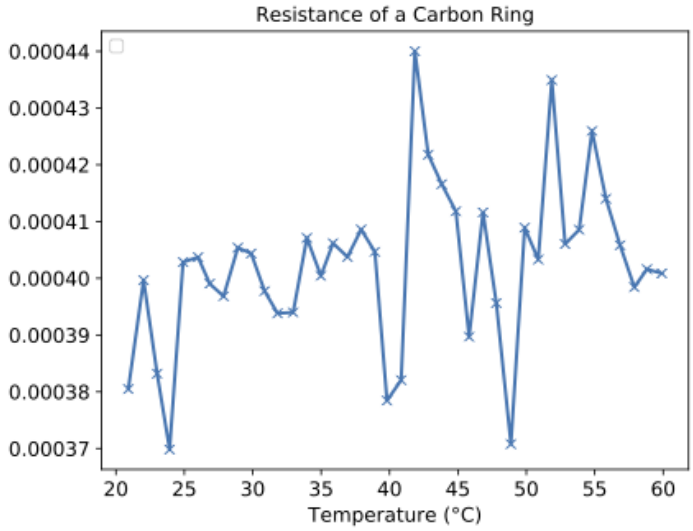

Figure 12: Resistance of a copper ring.

Fig. 10 represents the final sample of a copper ring with an average resistivity of 0.00053 Ω cm.

In Figure 10, the resistance for bare copper contacts displays a trend of

increasing resistance with some fluctuations as the temperature increases. These sharp fluctuations indicate that the thermal transport over the copper contacts may be due to the ring structure when 4-point measurements were being taken inside the climate chamber. Since the sample was not a copper thin film on a silicon substrate, the probes might have not been completely in contact with the physical structure of the ring without having a substrate layer. Thermal contact resistance is often observed on the applied force implemented rather than the available area for contact [26].

In terms of physical boundary, the heat carriers (in this case are the phonon scattering), will either reflect or transmit to the opposing interface. At the interface, an additional resistance is introduced to the heat flow called thermal boundary resistance. This transmission across the boundary would diffusely transmit heat carriers throughout the system [26], it is further shown from data oscillations of surface reflection that increase with wavelength.

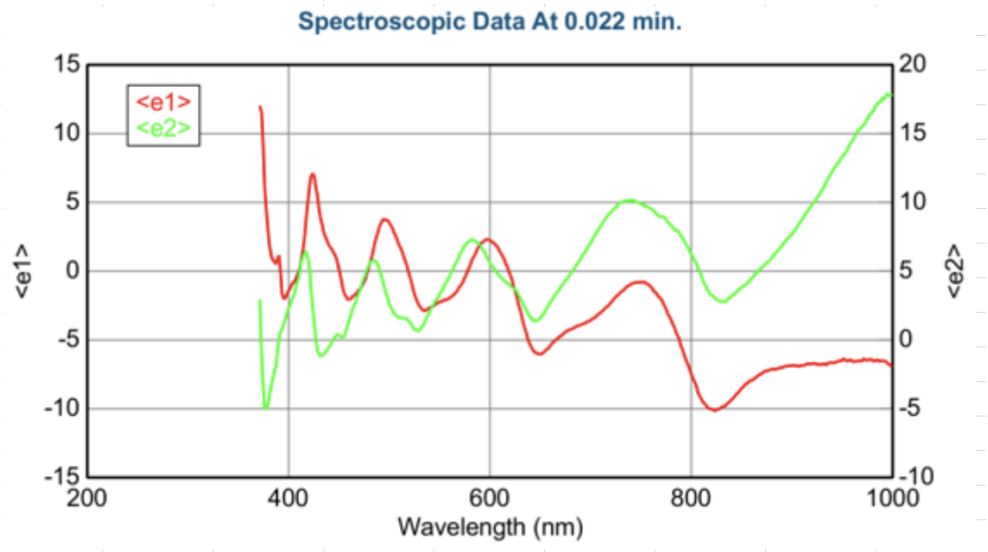

Figure 13: ϵ_1 and ϵ_2 spectra of copper.

As shown in the gold sample, the imaginary part of ϵ_2 for copper depicts similar increasing behavior and the real part of ϵ_1 decreases in behavior. There is a direct relation between the increase in temperature with longer wavelengths that describe this common behavior for metals.

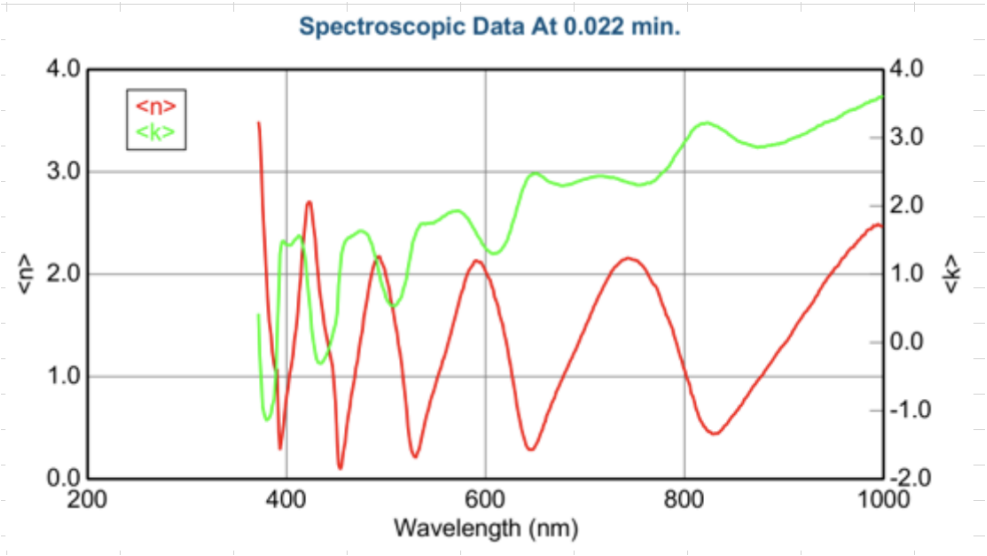

Figure 14: ϵ_1 and ϵ_2 spectra of copper.

The refractive index n of 0.950 gradually increased significantly with extinction coefficient k of 1.777 when measured at 550 nm. Fig.11 demonstrates the variation in the real part exhibiting a similar pattern to that of the imaginary part. Consistently, the real part exhibits lower values than the imaginary part. Notably opposed to the trend seen in Fig. 8, both the real and imaginary components of the dielectric constant exhibit an decrease as the photon energy rises.

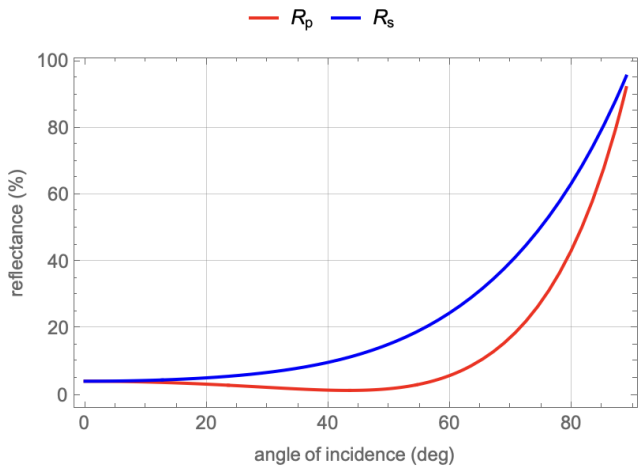

Figure 15: Reflectance of a thin film of copper on silicon substrate.

Fig.15, the reflectance percent at incident angle 70 is approximated to be 90 percent considering R_s. As the Fresnel amplitude and phase are changed due to temperature rise, we calculated $\epsilon = 2.028 + 0.637\text{i}$ which corresponds to $\tilde{n} = 0.950 + 1.777\text{i}$. Our findings are significantly lower when we compare $\tilde{n}$ value to the Wolfram graph [15], where $\tilde{n} = 0.676 + 2.624\text{i}$. When comparing the optical constants obtained from data analysis to the Brendel-Bormann model, our findings do not agree with the literature review. At approximately 550 nm, (n) of 0.676 with coefficient (k) of 2.624 [17] confirming that these estimations are exact to Wolfram values [15]. Other literature parameters denoted $\rho_p = 0.571$ and $\rho_s = 0.899$ with equal values and a model for reflectance from [17] is found to be similar to Fig. 14.

5 Conclusion

The investigation of the thermal properties of thin metal films were studied and in greater detail, for thermal reflectance both theoretically and experimentally using optical and electron microscopy techniques. The expected result was to measure the temperature dependence of the reflectance of metal films as a function of wavelength. Our experimental results indicate that temperature-dependent deviations in the metal optical constants were quite significant. In applications where electrical and optical properties are important; the film thickness for different metals plays an essential role in dictating the optimal functionality of ideal candidates that can measure thermal reflectance under susceptible temperatures. Since the thickness of films had approximately equal sizes, it largely contributed to the altercation of properties: resistivity, durability, optical wavelength, reflectivity and opacity. Similarly, the structure of the film depends on the substrate material; when the metal of choice coated indicates the binding forces between surface contacts can cause how well resistance is retained under thermal conditions. Another factor that may be considered is the phenomenon of charged carriers in an electric field scattering by the surface, which is responsible for when the film thickness is smaller than the mean free path. A similar trend observed from ellipsometry measurements attribute to characterization of optical responses of the thin films which may exhibit good thermal reflectance behavior if the thicknesses were larger than the experimental. As a result, thinner films have significant higher losses at elevated temperatures and fundamentally affects the behaviors in the optical constants observed that are not ideal. According to our experimental results, we can validate that gold and silver thin films on silicon substrate are the ideal candidates to investigate thermal properties of thin metal films under heating conditions due to gold's low contact resistance and high chemical stability and silver's superior

performance under extreme heating, respectively. However, according to literature values from Wolfram [15], aluminium is noted as the highest reflectance percent of 75 - 95 and Fig. 4 gives us a reflectance of 65 percent that is slightly below. It is noted that although prepared samples obtained had shown slight defects on their surface and degradation in the material that may have contributed to these losses, precise and careful manufacture of the films should be strongly considered to maximize optimization of functionality. This may be one of the few issues where our aluminium sample does not agree with the literature value leading to a minor fault in our findings. For future experiments, we can suggest future experiments that involve taking measurements at specific wavelengths to discern in detail and include delay times to compare these differences in thermoreflectance signals at timescales to differences in sensitivity after heating. Our findings demonstrated that the thickness of metal films significantly affects their thermal reflectance properties, giving further important insights for the design and optimization of metal films for applications where electric and optical properties undergo temperature related processes.

6 References

[1] Nanowerk. "MOF (metal-organic framework)." https://www.nanowerk.com/mof-metal-organic-framework.php.

[2] Babaei, H.; McGaughey, A. J. H.; Wilmer, C. E. Effect of Pore Size and Shape on the Thermal Conductivity of Metal-Organic Frameworks. Chem. Sci. 2017, 8, 583– 589, DOI: 10.1039/C6SC03704F [Crossref], [PubMed], [CAS], Google Scholar

[3] Howarth, A. J.; Liu, Y.; Li, P.; Li, Z.; Wang, T. C.; Hupp, J. T.; Farha, O. K. Chemical, Thermal and Mechanical Stabilities of Metal-Organic Frameworks. Nat. Rev. Mater. 2016, 1, 15018 DOI: 10.1038/natrevmats.2015.18

[4] Mason, J. A.; Sumida, K.; Herm, Z. R.; Krishna, R.; Long, J. R. Evaluating Metal-Organic Frameworks for Post-Combustion Carbon Dioxide Capture via Temperature Swing Adsorption. Energy Environ. Sci. 2011, 4, 3030– 3040, DOI: 10.1039/c1ee01720a

[5] Healy, Colm, et al. "The thermal stability of metal-organic frameworks." Coordination Chemistry Reviews, vol. 419, 2020, article no. 213388, ISSN 0010-8545, https://doi.org/10.1016/j.ccr.2020.213388.

[6] Han, L.; Budge, M.; Greaney, A. P. Relationship between Thermal Conductivity and Framework Architecture. Comput. Mater. Sci. 2014, 94, 292–297, DOI: 10.1016/j.commatsci.2014.06.008

[7] Howarth, A. J.; Liu, Y.; Li, P.; Li, Z.; Wang, T. C.; Hupp, J. T.; Farha, O. K. Chemical, Thermal and Mechanical Stabilities of Metal-Organic Frameworks. Nat. Rev. Mater. 2016, 1, 15018 DOI: 10.1038/natrevmats.2015.18

[8] Babaei, H.; McGaughey, A. J. H.; Wilmer, C. E. Effect of Pore Size and Shape on the Thermal Conductivity of Metal-Organic Frameworks. Chem. Sci. 2017, 8, 583– 589, DOI: 10.1039/C6SC03704F

[8] Maria Rosaria di Nunzio, Elena Caballero-Mancebo, Boiko Cohen, Ab-

derrazzak Douhal, Photodynamical behaviour of MOFs and related composites: Relevance to emerging photon-based science and applications, Journal of Photochemistry and Photobiology C: Photochemistry Reviews, Volume 44, 2020, 100355, ISSN 1389-5567, https://doi.org/10.1016/j.jphotochemrev.2020.100355. (https://www.sciencedirect.com/science/article/pii/S138955672030023X)

[9] Aaron J. Schmidt, Ramez Cheaito, Matteo Chiesa; Characterization of thin metal films via frequency-domain thermoreflectance. Journal of Applied Physics 15 January 2010; 107 (2): 024908. https://doi.org/10.1063/1.3289907

[10] R. B. Wilson, Brent A. Apgar, Lane W. Martin, and David G. Cahill, "Thermoreflectance of metal transducers for optical pump-probe studies of thermal properties," Opt. Express 20, 28829-28838 (2012)

[11] David H. Olson, Jeffrey L. Braun, Patrick E. Hopkins; Spatially resolved thermoreflectance techniques for thermal conductivity measurements from the nanoscale to the mesoscale. Journal of Applied Physics 21 October 2019; 126 (15): 150901. https://doi.org/10.1063/1.5120310

[12] R. Rosei and D. W. Lynch, "Thermomodulation Spectra of Al, Au, and Cu," Phys. Rev. B 5(10), 3883–3894 (1972).

[13] J.A. Woollam Co. Inc. "Ellipsometry Data Analysis."https://www.jawoollam.com/resources/ellipsomet tutorial/ellipsometry-data-analysis.

[14] Gilani, Tariq, and Diana Rabchuk. "Electrical Resistivity of Gold Thin Film." Canadian Journal of Physics, vol. 96, 2017, pp. 1156-1160, doi: 10.1139/cjp-2017-0484.

[15] "Fresnel Coefficients of Metals" http://demonstrations.wolfram.com/FresnelCoefficientsOfMetals/ Wolfram Demonstrations Project Published: August 31, 2020

[16] "Material Properties" https://iarc.uncg.edu/elight/learn/determine/lc$_s ub/mat_p rop.html$

[17] A. D. Rakić, A. B. Djurišic, J. M. Elazar, and M. L. Majewski. Optical properties of metallic films for vertical-cavity optoelectronic devices, Appl. Opt.

37, 5271-5283 (1998)

[18] Mirigliano, Mariella, et al. "Anomalous electrical conduction and negative temperature coefficient of resistance in nanostructured gold resistive switching films." Scientific Reports, vol. 10, 2020, article no. 19613, https://doi.org/10.1038/s41598-020-76632-y.

[19] Czerwinski, Felix. "Thermal Stability of Aluminum Alloys." Materials, vol. 13, no. 15, 2020, article no. 3441, doi: 10.3390/ma13153441.

[20] Favaloro, T., Je-Hyeong Bahk, and Ali Shakouri. "Characterization of the temperature dependence of the thermoreflectance coefficient for conductive thin films." Review of Scientific Instruments, vol. 86, 2015, article no. 024903, doi: 10.1063/1.4907354.

[21] Yajadda, Mirza M. A., et al. "Effect of Coulomb Blockade, Gold Resistance, and Thermal Expansion on the Electrical Resistance of Ultrathin Gold Films." Physical Review B, vol. 84, no. 23, 2011, article no. 235450, https://doi.org/10.1103/PhysRevB.84.235450.

[22] Reddy, Harsha, et al. "Temperature-dependent optical properties of gold thin films." Optical Materials Express, vol. 6, no. 8, 2016, pp. 2776-2802, doi: 10.1364/OME.6.002776.

[23] Kim, H. C., T. L. Alford, and D. R. Allee. "Thickness dependence on the thermal stability of silver thin films." Applied Physics Letters, vol. 81, no. 22, 2002, pp. 4287-4289, doi: 10.1063/1.1525070.

[24] Kawamura, M., et al. "Metal nanolayer deposited highly stable Ag thin films and their optical properties." Journal of Physics: Conference Series, vol. 987, 2018, article no. 012002, doi: 10.1088/1742-6596/987/1/012002.

[25] Kudo, Eita, et al. "Optical properties of highly stable silver thin films using different surface metal layers." Thin Solid Films, vol. 660, 2018, pp. 730-732, doi: 10.1016/j.tsf.2018.03.086.

[26] Dhuley, Ram. (2019). Pressed copper and gold-plated copper contacts at low temperatures - A review of thermal contact resistance. Cryogenics. 101. 10.1016/j.cryogenics.2019.06.008.